Potential Impacts of polypropylene Microplastics on the Adsorption Process of Cr(VI) by Biochar

Ho Truong Nam Hai[1,3], Pham Thi Phuong Le[1,3], Nguyen Thao Nguyen[1,3], Nguyen Thi Thanh Nhon[1,3], Nguyen Tran Hanh Vy[2,3], Tan Le Hoang Doan[2,3], To Thi Hien[1,3,*]

[1]Faculty of Environment, University of Science, Ho Chi Minh City, Vietnam
[2]Center for Innovative Materials and Architectures, Ho Chi Minh City, Vietnam
[3]Vietnam National University, Ho Chi Minh City, Vietnam
Email: htnhai@hcmus.edu.vn (H.T.N.H.); phamphuongle3001@gmail.com (P.T.P.L.); ngtnguyen@hcmus.edu.vn (N.T.N.); nttnhon@hcmus.edu.vn (N.T.T.N.); nthvy@inomar.edu.vn (N.T.H.V.); dlhtan@inomar.edu.vn (T.L.H.D.); tohien@hcmus.edu.vn(T.T.H.)
ORCID: 0000-0001-8804-6166 (H.T.N.H.); 0000-0002-2782-5681 (N.T.N.); 0000-0003-0497-0381 (N.T.T.N.); 0000-0001-6312-9571 (T.L.H.D.); 0000-0003-2631-4123 (T.T.H.)

[*]Corresponding author

Manuscript received January 28, 2024; revised May 17, 2024; accepted June 28, 2024; published October 14, 2024

***Abstract*—Microplastics are a serious concern today because of their huge quantities in the environment, their ability to adsorb toxins on surfaces, their ease of entry in the food chain based on micron size, and theirs contributing to increased potential health threats. However, a new aspect of microplastics' presence impacting the pollutant treatment efficiency is poorly understood. This study clarifies the effects of microplastics on the adsorption process of Cr(VI) by biochar, an effective and inexpensive material for wastewater treatment. Techniques such as Fourier Transform Infrared (FTIR) Spectroscopy, Nitrogen adsorption/ desorption, and Scanning Electron Microscope (SEM) were used to assess the characteristics of adsorbents. The results showed that biochar had a large surface area and pore volume (313.91 m^2/g; 0.45 cm^3/g); these values were significantly higher than polypropylene microplastics (7.04 m^2/g; 0.007 cm^3/g). Biochar's pores were mainly micropores (less than 2 nm), while polypropylene's ones were mesopores (2 to 50 nm). Batch experiments were conducted following the influencing factors. Adsorption data indicated that Freundlich, Sips, and Redlich-Peterson isotherms were suitable for Cr(VI) adsorption by biochar. The Freundlich and Redlich-Peterson isotherms described well the adsorption of Cr(VI) well by the mixture of biochar and polypropylene microplastics. For kinetic data, second-order kinetics was more suitable than first-order kinetics for Cr(VI) adsorption onto the materials. The Elovich diffusion and liquid film diffusion models are suitable for describing the adsorption pathway of Cr(VI) on a mixture of microplastics and biochar. In conclusion, microplastics significantly affect the adsorption of Cr(VI) by biochar.**

***Keywords*—adsorption, biochar, Cr(VI), microplastics, polypropylene**

I. Introduction

Rapid industrialization requires various chemicals in production, leading to industrial wastewater containing many persistent organic compounds and a large amount of heavy metals that are difficult to treat [1]. Various technologies, such as electrolysis, ion exchange, reverse osmosis, membrane separation, and adsorption, have been widely employed to treat metals wastewater, depending on their applicability and initial pollutant concentration. Among these techniques, adsorption is a straightforward, efficient, and cost-effective method of metals removal [2–4].

In metals-containing effluents, pollutants can originate from various sources, such as solids, dissolved substances, microorganisms, and microplastics. Microplastics are an emerging pollutant and have become a global concern [5]. Microplastics possess a high surface area-to-volume ratio, enabling the adsorption and accumulation of chemical contaminants, including heavy metals, inorganics, and persistent organic pollutants [6, 7]. Microplastics play a role as vectors, introducing pollutants into the food chain and subsequently affecting the environment and humans [8].

Recent studies have focused on monitoring microplastics in air, water, soil, and also creatures, as well as, the adsorption of pollutants onto microplastics; and the effectiveness of microplastic removal in wastewater treatment systems [4, 5, 9, 10]. However, considering the impact of microplastics on the effectiveness of other pollutant treatment in wastewater is a new aspect that needs to be approached. Regarding microplastics as potential adsorbents, the presence of microplastics will possibly compete with other adsorbents in the adsorption process. Through our investigation, we will provide insights into the environmental behavior of microplastics by mixing biochar and microplastics into a mixture that is not chemically bonded. This will clarify the efficacy of adsorbing metal in water where adsorbent and microplastics coexist.

II. Literature Review

Chromium, a widely used metal in industry, is a hazardous contaminant that exists in various oxidation states. The two most popular oxidation states of chromium are Cr(III) and Cr(VI), with Cr(VI) being 300 times more toxic than Cr(III) and classified as a carcinogenic and genotoxic compound [11, 12]. Chromium ranks as the second most common human skin allergen (after nickel), and large doses of Cr(VI) entering the bloodstream can cause liver and kidney damage, including acute tubular necrosis [13]. The average concentration of chromium in the Earth's crust is 125 mg/kg, approximately 11 to 22 mg/kg in soil, 1 μg/L in surface water, and 100 μg/L in groundwater [14]. The prescribed range for industrial wastewater, according to QCVN 40:2021/BTNMT, is 0.05 to 0.1 mg/L (Vietnam National Technical Regulation on industrial wastewater). Due to its high toxicity, chromium-containing effluents must undergo proper treatment before being discharged into the environment.

Since the widespread production of plastic products in the

1950s, plastic waste and microplastics have been accumulating in earthly, oceanic, and atmospheric environments [10]. The quantity of microplastics is on the rise due to the release and dispersion of plastic particles during production and transportation, the continuous fragmentation of large pieces of plastic, and the inherent properties of durability, light weight, and mobility [15]. Murphy's research demonstrated that over 65 million microplastic pieces are discharged daily from wastewater treatment plants [16]. Simon's study at a Danish treatment plant estimated an annual release of 3 tons of microplastics ranging from 10 to 500 μm [17]. The majority of microplastics in wastewater are polypropylene (PP) [10]. In Long's study conducted at a wastewater treatment plant in Xiamen, China, the proportion of PP ranged from 20.4% to 41.6% [9]. Recent research has shown the ability of microplastics to adsorb heavy metals [6, 18]. Considering that PP is a potential absorbent, its presence could influence the efficiency of adsorption when using biochar as the primary method for removing chromium from effluents [15].

Peanut shells constitute 25–30% of peanut products, and global peanut production reached an estimated 43.98 million tonnes in 2016, indicating that making biochar derived from peanut shells could effectively capture carbon from biomass [19]. Besides, biochar derived from peanut shells possesses considerable potential for the treatment of heavy metal-contaminated wastewater through adsorption, owing to its abundant functional groups, pores, and high specific surface area [15].

The study was carried out in batches, considering the optimal influent parameters (pH, contact time, adsorbent mass, and initial Cr(VI) concentration) of biochar and the mixture of biochar and microplastics. This study aimed to investigate the effect of PP on the adsorption of Cr(VI) by biochar.

III. Materials and Methods

A. Chemicals and Materials

All chemicals used in this study were analytical reagents. To prepare the chromium(VI) stock solution, 1.417 g of pre-dried potassium dichromate (CAS Number: 7778–50–9, Sigma – Aldrich) was dissolved in 500 mL of deionized water. Working solutions were diluted from the stock solution to the required concentration. Two solutions (HCl or NaOH) at two different concentrations (2.5N and 0.5N) were used by adding to the working solution to reach a desired pH value. Reagent solution was obtained by dissolving 1.0 g of 1,5-Diphenylcarbazide (CAS Number: 140–22–7, Merck) in 100 mL of acetone solution, adding one drop of acetic acid and storing it refrigerated at 4°C.

B. Adsorbent Preparation

Biochar making was modified based on Georgin's research [20]. First, peanuts were purchased from Khiet Tam Market, Thu Duc City, Viet Nam (10°52'36.27"N, 106°44'48.67"E). In the laboratory, peanut shells were separated, chopped, and washed three times with distilled water. Subsequently, they were dried in an oven at 60°C for 24 hours. The dried shells were filled into a crucible with a tight lid and put into a kiln (Daihan Fx–03, Korea). When the kiln reached a temperature of 600°C, the slow pyrolysis process occurred in an anoxic environment over 2 hours. After the process ended, the incompletely calcined part was removed. Next, the biochar was crushed and passed through two sieves with pore sizes of 0.25 mm and 0.1 mm. Washing the biochar three times with distilled water and drying it at 60°C for 24 hours ensures no interference from microplastics in the fabric and equipment from the experiment into the sample. Finally, the biochar was stored in a glass bottle at 4°C.

Polypropylene fragments (5–10 mm) used in this study were obtained from a local plastic manufacturer located in Ho Chi Minh City, Viet Nam (10°46'11.52"N, 106°34'15.10"E). During the pre-treatment stage, the fragments were subjected to ball milling and passed through sieves with 0.25 mm and 0.1 mm pore sizes. The microplastics collected on the 0.1 mm sieve were washed three times with distilled water, filtered through vacuum filtration system, and dried thoroughly in an oven at 60°C for 48 hours. They were subsequently stored in a glass bottle at 4°C until further use.

C. Properties of Adsorbents

The characteristics of biochar and PP were analyzed using several methods. FTIR (FTIR - 6600 type A, Jasco, Hachioji, Tokyo, Japan) was employed with 32 scans/spectrum in the wavelength 497.54–4003.5 cm^{-1} to determine the functional groups of samples. The surface of samples was observed using a SEM (JSM–6400, Jeol, Japan) with an acceleration voltage of 5 kV. The point of zero charge (pH_{pzc}) of the adsorbent was determined following method described in Al-Maliky's research [21]. The surface area and pore characteristics of the material were determined using the Brunauer–Emmett–Teller (BET) method on the equipment (Nova Station A, Quantachrome, USA). The samples were subjected to N_2 adsorption at 77.350 K and degassed under vacuum conditions at 573 K. The BET equation was used to establish the relationship between the pressure (P/P_o), which ranged from 0.01 to 0.3. After the sorption tests, the microplastics were separated by density using NaCl-saturated solution while biochar was filtered through filter paper (Qualitative Filters Papers 5A, 110mm, Advantec, Japan). Each part of biochar and microplastics was dried completely in an oven at 60°C for 48 hours and stored in a glass bottle at 4°C for subsequent analysis alongside the pre-samples for the aforementioned parameters.

D. Batch Adsorption Tests

To determine the optimal parameters for Cr(VI) adsorption by biochar, batch experiments were undertaken. The conditions for each experiment are detailed in Table A1. Subsequently, the influence of PP on Cr(VI) adsorption by biochar was examined through batch experiments using the optimal conditions mentioned above. These experiments are described in Table B1.

The experiment involved adding a specific volume of Cr(VI) solution with a known concentration to an Erlenmeyer flask. The pH of solution was adjusted using HCl or NaOH solutions to the desired pH value. Then, the

appropriate amount of adsorbent (either biochar or mixture of PP and biochar) was added to the solution. The Erlenmeyer flask was shaken at room temperature using equipment (SCI–L330–Pro, Scilogex, USA). After the designated reaction time, the mixtures were filtered through filter paper. The Cr(VI) concentration in the filtrate was analyzed by measuring the absorbance of the Cr(VI) complex at the maximum absorption wavelength of 540 nm using UV-Vis equipment (V650, Jasco, Japan) [22].

The adsorption capacity at equilibrium (q_e) was determined using Eq. (1), which is used to calculate Freundlich and Langmuir adsorption isotherms. Eq. (2) describes the processing efficiency (%R). The experiments were replicated three times to obtain the average result.

$$q_e = \frac{V(C_o - C_e)}{m} \quad (1)$$

$$\%R = \frac{(C_o - C_e)}{C_0} \quad (2)$$

where V is the volume of solution (L), m is the amount of adsorbent (g), C_o is the initial Cr(VI) concentration in liquid phase (mg/L), and C_e is the equilibrium Cr(VI) concentration in the liquid phase (mg/L).

E. Kinectic and Isotherm Studies

The kinetics of the adsorption of Cr(VI) onto biochar and the mixture of biochar and PP were considered using 75 mg/L Cr(VI). Additionally, isotherm models (Redlich-Peterson, Sips) were employed to elucidate the molecule distribution between the Cr(VI) ion and the solid phase at the equilibrium time. Table C1 describes the models used in the study. To verify the suitability of these models, the coefficients of determination R^2 and Average relative error (ARE) are calculated based on Eqs. (3), (4).

$$R^2 = 1 - \frac{\sum(q_{e,exp} - q_{e,cal})^2}{\sum(q_{e,exp} - q_{e,mean})^2} \quad (3)$$

$$ARE = \frac{100}{N}\sum_{i=1}^{N}\left|\left(\frac{q_{e,cal} - q_{e,exp}}{q_{e,exp}}\right)\right|_i \quad (4)$$

where $q_{e,exp}$, $q_{e,cal}$, and $q_{e,mean}$ are the experimental, caculated, and average adsorption capacities, respectively. N is the number of experimental data.

F. Quality Control

To determine whether Cr(VI) is present in biochar and PP, an experiment was conducted by adding a mixture of biochar and PP (0.05g: 0.05g) to deionized water without any initial Cr(VI) concentration at different pH values: 2, 4, 6, 8, 10, 12 with the stirring of 200 rpm in 120 minutes (as blank control #1). The experiment showed no contamination of Cr(VI) from the adsorbents. Additionally, the recovery of Cr(VI) during adsorption process was evaluated by using an initial Cr(VI) concentration of 50 mg/L without the addition of any adsorbent (as blank control #2). The result showed that the average sample recovery was 98.5 $\pm$ 0.6%.

IV. Results And Discussion

A. Adsorbent Characterization

Before adsorption, biochar exhibited a rough surface and numerous pores (Fig. 1a). In contrast, the surface of the PP microplastics was relatively flat, and the number of pores was negligible (Fig. 1c). These findings are consistent with the results presented in Table 1, which show that the surface area and pore volume of biochar are significantly higher than those of PP. After Cr(VI) adsorption, the biochar surface became smooth, and the pores were filled (Fig. 1b). As for PP, its surface showed little significant difference compared to pre-adsorption (Fig. 1d). However, in the mixture of biochar and PP after adsorption, the surface of PP became more irregular, and crystalline debris appeared on its surface (Fig. 1e). While biochar's surface was not completely filled, in contrast to the adsorption process with only biochar (Fig. 1f). Therefore, PP may hinder the adsorption Cr(VI) of biochar.

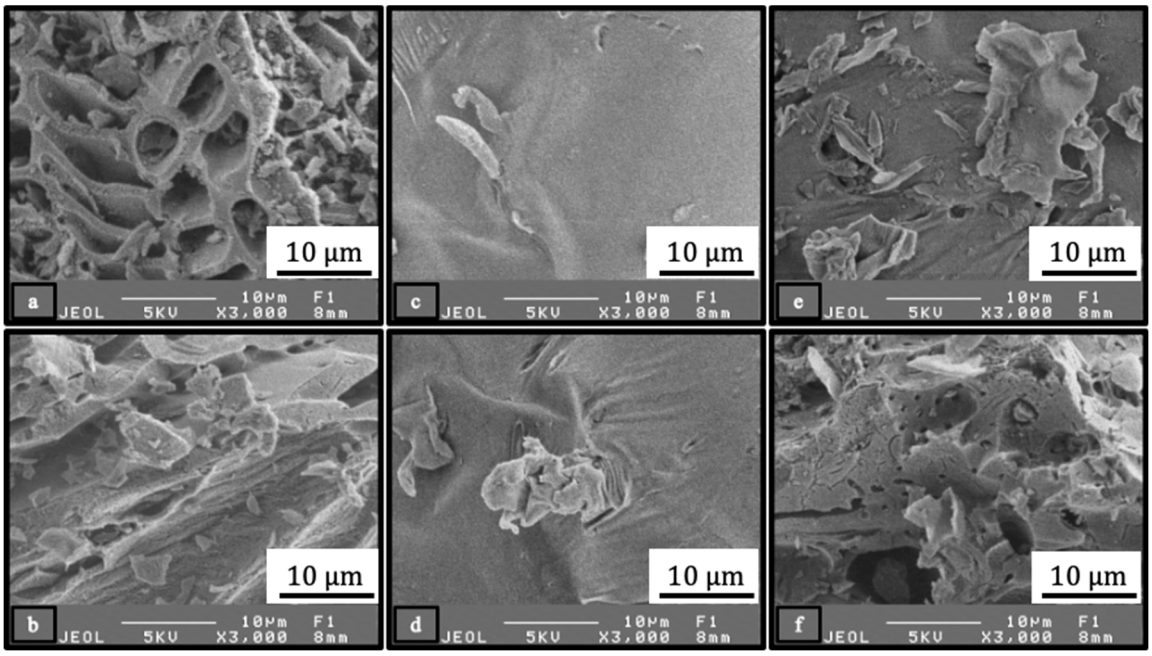

Fig. 1. SEM image for (a) biochar before adsorption; (b) biochar after adsorption; (c) PP before adsorption; (d) PP after adsorption; (e) PP in the mixture after adsorption; (f) biochar in the mixture after adsorption.

Table 1. Pore structure of biochar and PP. St, Vt, and Dt represent the surface area, pore volume, and pore diameter. SBET represents the surface area determined by the BET method

Material	S_{BET} (m^2/g)	S_t (m^2/g)	V_t (cm^3/g)	D_t (nm)
Biochar	313.91	156.06	0.45	1.43
PP	7.04	7.61	0.007	2.46

The BET surface area of biochar and PP was 313.91 and 7.04 m^2/g, respectively (Table 1). Biochar's pores were mainly micropores (less than 2 nm), while PP's ones were mesopores (2–50 nm) [23]. Fig. 2 depicts the N_2 adsorption-desorption isotherms of adsorbents. The isotherm for biochar exhibited type II adsorption, indicating unrestricted monolayer-multilayer adsorption and non-porous adsorbent [24]. Conversely, the isotherm of PP displayed a linear pattern that does not conform to any isotherm based on the International Union of Pure and Applied Chemistry (IUPAC) classification system. These characteristics analyse may explain the higher uptake of Cr(VI) by biochar due to higher specific surface area and pore volume. However, PP microplastic may also adsorb Cr(VI) at mesopore sites on its surface.

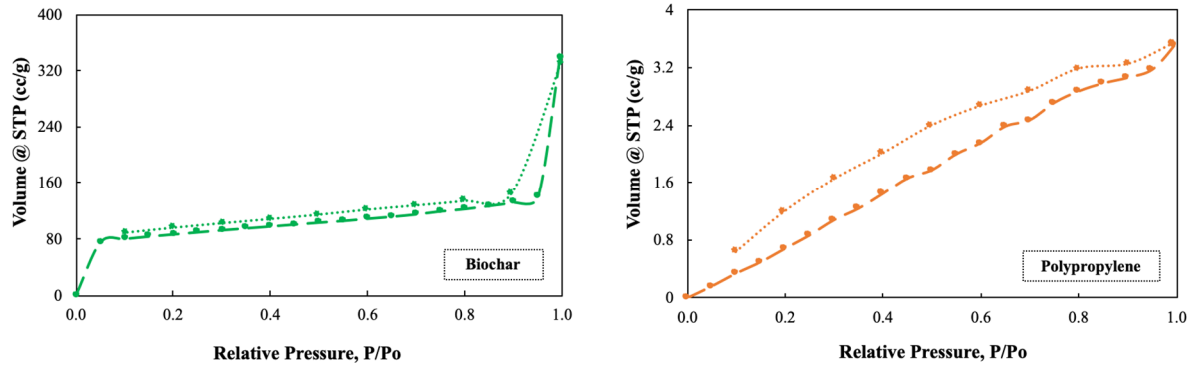

Fig. 2. N_2 adsorption-desorption isotherms of the biochar and polypropylene.

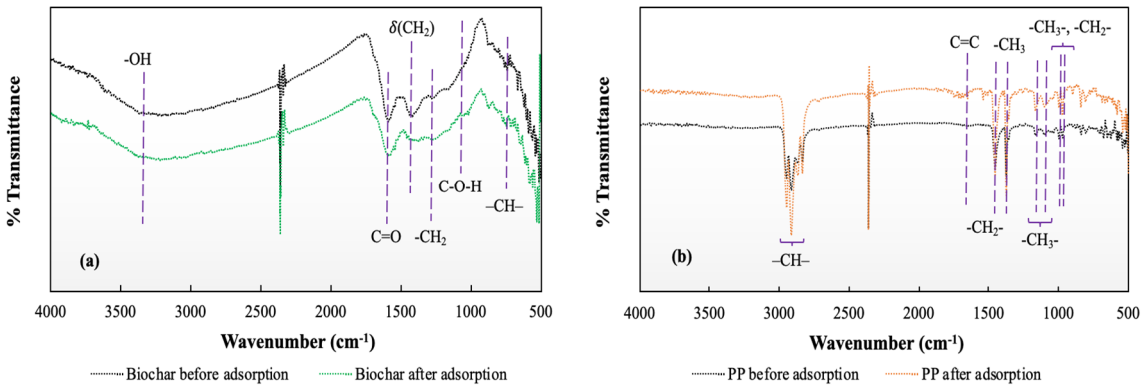

Fig. 3. IR spectra of (a) biochar, (b) PP before and after adsorption.

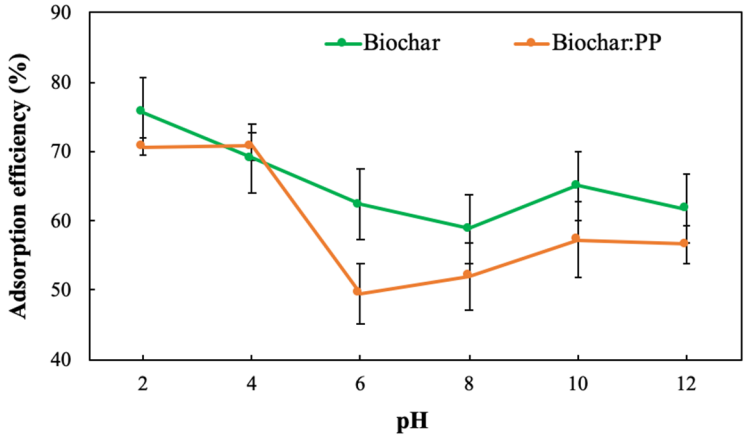

Fig. 4. Effect of pH for the adsorption of Cr(VI) on biochar and the mixture of biochar and PP (1:1) [*Initial Cr(VI) concentration 50 mg/L; solution volume 50 mL; adsorbent mass 0.1 g; time 120 minutes; stirring speed 200 rpm*].

Fig. 3a illustrates IR spectra of biochar before and after the adsorption process. The results show a peak at 3350 cm^{-1}, typical for single bond O-H stretch. Additionally, there is a peak at 1592 cm^{-1} attributed to the elongated C=O bond resulting from carboxyl groups (-COOH, -$COOCH_3$) and aldehydes from quinine, lactone, carboxylic acid, and hemicellulose. Another peak of 1429 cm^{-1} represents the characteristic $\delta(CH_2)$ vibration of polysaccharides and cellulose, while a fluctuation at 743 cm^{-1} is described as an aromatic extension of –CH–. Overall, these results indicate

that biochar surface is predominantly covered by aromatic functional groups [25]. After Cr(VI) adsorption, some changes in the spectrum are observed, with a weaker fluctuation at 1429 cm^{-1} and the appearance of a peak at 1076 cm^{-1} (C–O–H) in the IR spectrum of biochar. These changes can be attributed to the presence of Cr(VI) ions ($Cr_2O_7^{2-}$, $HCrO_4^-$) and H^+ ions, which undergo ion exchange with the biochar surface. These findings align with previous studies of grass, wood, and manure-based biochars [11, 25].

Fig. 3b illustrates FTIR spectrum of PP microplastics before and after adsorption. The peaks observed at 2950 cm^{-1}, 2218 cm^{-1}, 2868 cm^{-1}, 2839 cm^{-1} are characteristic of -CH- bond stretching. A peak at 1457 cm^{-1} represents the -CH_2 bending vibration, while a peak at 1376 cm^{-1} corresponds to the -CH_3 bending vibration. Peaks at 1167 cm^{-1} and 1107 cm^{-1} indicate symmetric deformation vibrations of –CH_3-. Additionally, peaks at 998 cm^{-1} and 973 cm^{-1} correspond to the rocking vibrations of –CH_3- and –CH_2- groups, respectively. These characteristic peaks confirm the presence of polypropylene [26]. After adsorption, the FTIR spectrum of PP shows the detection of a C=C double bond at the peak of approximately 1601 cm^{-1} [27].

B. *Effect of pH*

The influence of pH on the Cr(VI) adsorption process is plotted in Fig. 4. In the case of adsorption with biochar alone, the highest adsorption efficiency was achieved at pH 2, reaching 75.6%. This can be attributed to the predominance of $HCrO_4^-$ and $Cr_2O_7^{2-}$ forms of Cr(VI) ions in the pH range of 2 to 6 in the solution [3]. Based on Fig. A1, the pHpzc of biochar derived peanut shells was determined to be 7.36. Therefore, in an acidic environment, biochar surface will attract positively charged functional groups. This finding suggests that a pH of 2 is necessary to create electrostatic attraction for adsorption of Cr(VI) ions. Additionally, the reduction process from Cr(VI) to Cr(III) facilitated by an adjacent electron donor, as described in Eqs. (5) and (6), also contributes to the decrease in Cr(VI) concentration in solution [2, 28]. At higher pH levels, the treatment efficiency decrease due to the formation of electrostatic repulsion between Cr(VI) ions and adsorbent surface, along with electrostatic competition between Cr(VI) anions and hydroxyl ions (OH^-) at adsorption sites [29].

$$Cr_2O_7^{2-} + 14H^+ + 6e^- \rightarrow 2Cr^{3+} + 7H_2O \quad (5)$$

$$HCrO_4^- + 3e^- + 3H_2O \rightarrow Cr^{3+} + 7OH^- \quad (6)$$

When microplastics were present during Cr(VI) adsorption onto biochar, the Cr(VI) removal efficiency was approximately the same at pH 2 and 4. This is comparable to the treatment efficiency observed when only biochar was present at pH 4. In this study, the pHpzc of PP was determined to be 4.49 (Fig. B1), which is consistent with a previous finding by Xu (pHpzc = 4.26) [30]. Despite being a non-biodegradable and chemically inert microplastic, the surface of PP retains water molecules, forming a layer of H^+ ions that enables electrostatic interactions with Cr(VI) anions (occurring at pH < pHpzc). This process may serve as the primary mechanism of Cr(VI) ion adsorption onto microplastic [18].

C. *Effect of Contact Time*

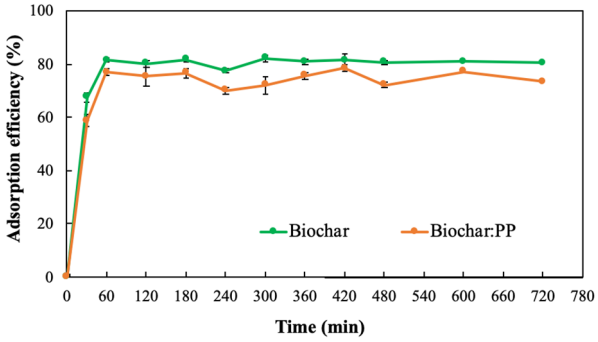

Fig. 5. Effect of time for the adsorption of Cr(VI) on biochar and the mixture of biochar and PP (1:1) [*pH 2; Initial Cr(VI) concentration 50 mg/L; solution volume 50 mL; adsorbent mass 0.1 g; stirring speed 200 rpm*].

Fig. 5 illustrates the adsorption equilibrium time of Cr(VI) on adsorbents. While the adsorption tendencies were quite similar, the presence of PP resulted in a reduction of 3 - 10% in treatment efficiency compared to biochar alone. Moreover, the adsorption equilibrium time varied between the two cases. The mixture of biochar and microplastic required 420 minutes (R = 78.3%), which was slower than biochar at 300 minutes (R = 82.1%). This difference can be attributed to the competitive adsorption between biochar and PP for Cr(VI) ions. The adsorption performance curve of the mixture of biochar and PP shows a strong reversible process at the equilibrium point involving adsorption and desorption of Cr(VI) ions. This can be attributed to the outer-sphere complexation of Cr(VI) adsorption on PP surface. This complexation occurs through the binding of sorbing ions to the hydrate layer of water molecules and is influenced by the surface functional group of PP [2]. This rapid and reversible process makes it easier for Cr(VI) ions to be released compared to direct ion binding to the functional group sites of biochar.

D. *Effect of Adsorbent Mass and the Ratio of Biochar to PP*

Fig. 6a displays the relation between biochar mass and adsorption efficiency. In the range of 0.05 and 0.1 g biochar mass, there was a significant increase in treatment efficiency from 67.4% to 81.7%. Beyond that, the treatment capacity exhibited a gradual increase. With each additional 0.05 g biochar, the percentage of Cr(VI) removal increased by 5% until reaching 0.3 g (98.1%). The maximum efficiency was achieved at 0.4 g (99.7%). As the amount of biochar increased, the available adsorption sites also expanded accordingly, while the concentration of Cr(VI) ions in solution remained constant [29].

The total mass of adsorbent used to investigate the influence of ratio (biochar:PP) on Cr(VI) removal efficiency was 0.4 g. Fig. 6b demonstrates that with the same mass of adsorbent, treatment efficiency declined as the ratio of biochar to PP decreased or as the mass of PP increased. The highest processing efficiency was achieved at a ratio of 9:1 (94.4%), while it decreased by approximately 20% to 73.8% at a ratio of 1:9. Therefore, PP shows some usefulness in adsorbing Cr(VI) ions in the solution but notably less effective compared to biochar.

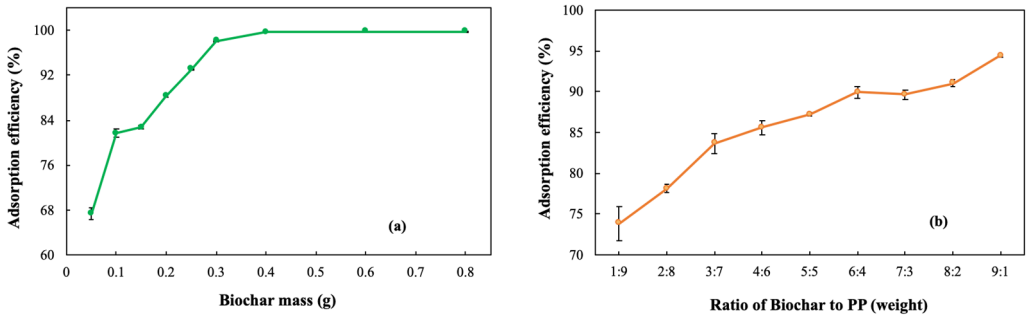

Fig. 6. (a) Effect of adsorbent mass for the adsorption of Cr(VI) on biochar [*pH 2; Initial Cr(VI) concentration 50 mg/L; solution volume 50 mL; time 300 minutes; stirring speed 200 rpm*]. (b) Effect of ratio of biochar to PP (weight) for the adsorption of Cr(VI) [*pH 2; Initial Cr(VI) concentration 50 mg/L; solution volume 50 mL; total mass 0.4 g; time 300 minutes; stirring speed 200 rpm*].

E. Effect of initial Cr(VI) Concentration

Fig. 7 illustrates adsorption process of Cr(VI) at various concentrations onto biochar. The removal percentage of Cr(VI) by biochar remained nearly constant in the initial concentration range of 25 mg/L to 75 mg/L (99.4%–98.2%, respectively). However, the treatment performance significantly decreased to the lowest value of 89.5% at 150 mg/L. On the one hand, the increasing Cr(VI) concentration results in a rising mass gradient between solution and adsorbents, facilitating the transfer of Cr(VI) molecules to the adsorbent surface [31]. On the other hand, the available adsorption sites on biochar surface gradually become saturated. With higher concentrations of Cr(VI), there are no vacant sites to bind the adsorbate [32].

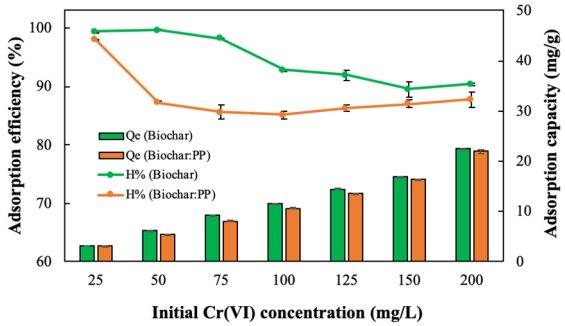

Fig. 7. Effect of initial Cr(VI) concentration for the adsorption of Cr(VI) on biochar and the mixture of biochar and PP (1:1) [*pH 2; solution volume 50 mL; adsorbent mass 0.4 g; time 300 minutes; stirring speed 200 rpm*].

For Cr(VI) adsorption with biochar and PP, removal efficiency exceeded 98% at an initial Cr(VI) concentration of 25 mg/L. However, as the initial Cr(VI) concentration increased, the removal performance sharply reduced compared to the trend observed with biochar alone (approximately 86%). This indicates that PP is ineffective in adsorbing Cr(VI) when the initial Cr(VI) concentrations are above 25 mg/L. The adsorption efficiency slightly increased from 85.1 to 87.8% when the Cr(VI) concentration rose from 100 to 200 mg/L. This change can be explained by the increased Cr(VI) concentration leading to more contact between Cr(VI) and the microplastic surface, thereby forming an adsorbate multilayer. However, this process is insignificant when the performance change is small and the desorption happens simultaneously. Fig. 7 also describes a positive correlation between adsorption capacity of adsorbents and initial Cr(VI) concentration. Under the same experimental conditions, the adsorption capacity of biochar remained higher than that of a mixture of biochar and microplastics.

F. Adsorption Isotherm

From Table 2 and Fig. 8, for the Cr(VI) adsorption process by biochar, the Sips and Redlich-Peterson models both had an R^2 coefficient of 0.999. Besides, the ARE of the Sips model was 17.9 while the Redlich-Peterson model was 18.19. Considering the above values, it shows that these two models both described the experimental adsorption data well and the Sips model performs was better. The m_s value of the Sips model was relatively high, 3.03, indicating that the system was heterogeneous. This is consistent with the Freundlich model since Freundlich's R^2 was 0.89 and the ARE value was equivalent. Langmuir's R^2 was 0.902, however Langmuir's ARE coefficient was 32.9, almost double that of Freundlich's ARE. The experimental adsorption amount at equilibrium was higher than the value of the maximum adsorption capacity from the Langmuir equation. Therefore, the Langmuir model is not suitable to describe the equilibrium isotherm.

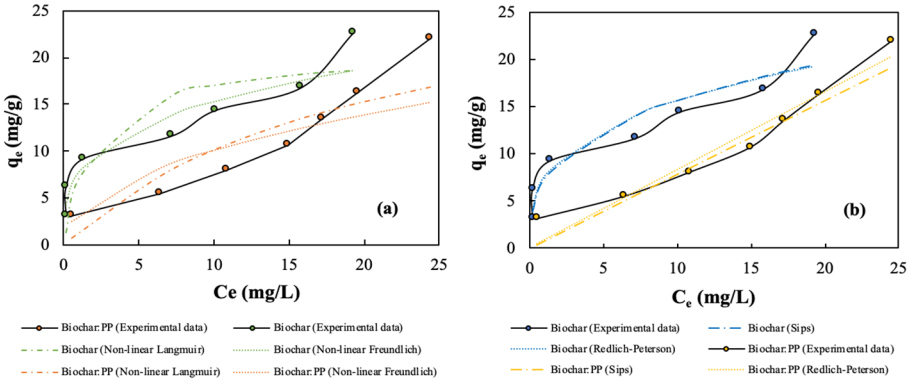

Fig. 8. Comparison between the experimental and predicted isotherms: (a) two-parameter isotherm (Langmuir, Freundlich) and (b) three-parameter isotherm (Sips, Redlich-Peterson) for the adsorption of Cr(VI) by biochar and the mixture of biochar and PP (1:1) [*pH 2; solution volume 50 mL; adsorbent mass 0.4 g; time 300 minutes; stirring speed 200 rpm*].

Table 2. Langmuir, Freundlich, Sips, and Redlich-Peterson isotherm constant for the adsorption of Cr(VI) on biochar and the mixture (biochar and PP)

Isotherm model	Parameters	Values	
		Biochar	Biochar:PP (1:1)
Langmuir	q_m (mg/g)	20.75	31.15
	K_L ((mg/g)/(mg/L)$^{1/n}$)	0.46	0.05
	R_L	0.01–0.08	0.09 – 0.45
	R^2	0.9	0.38
	ARE	32.9	28.8
Freundlich	K_F (L/mg)	7.67	3.47
	1/n	0.3	0.46
	R^2	0.89	0.83
	ARE	17.9	23.2
Sips	q_{m_S} (mg/g)	1780.6	2305.3
	K_S (L. mg^{-1})^{m_S}	0.004	0.0003
	m_S	3.03	1
	R^2	0.999	0.94
	ARE	17.9	18.5
Redlich-Peterson	K_R (L.g^{-1})	89638.8	1.37
	a_R (L.mg^{-1})	11926.6	0.66
	n	0.68	0
	R^2	0.999	0.997
	ARE	18.19	18.73

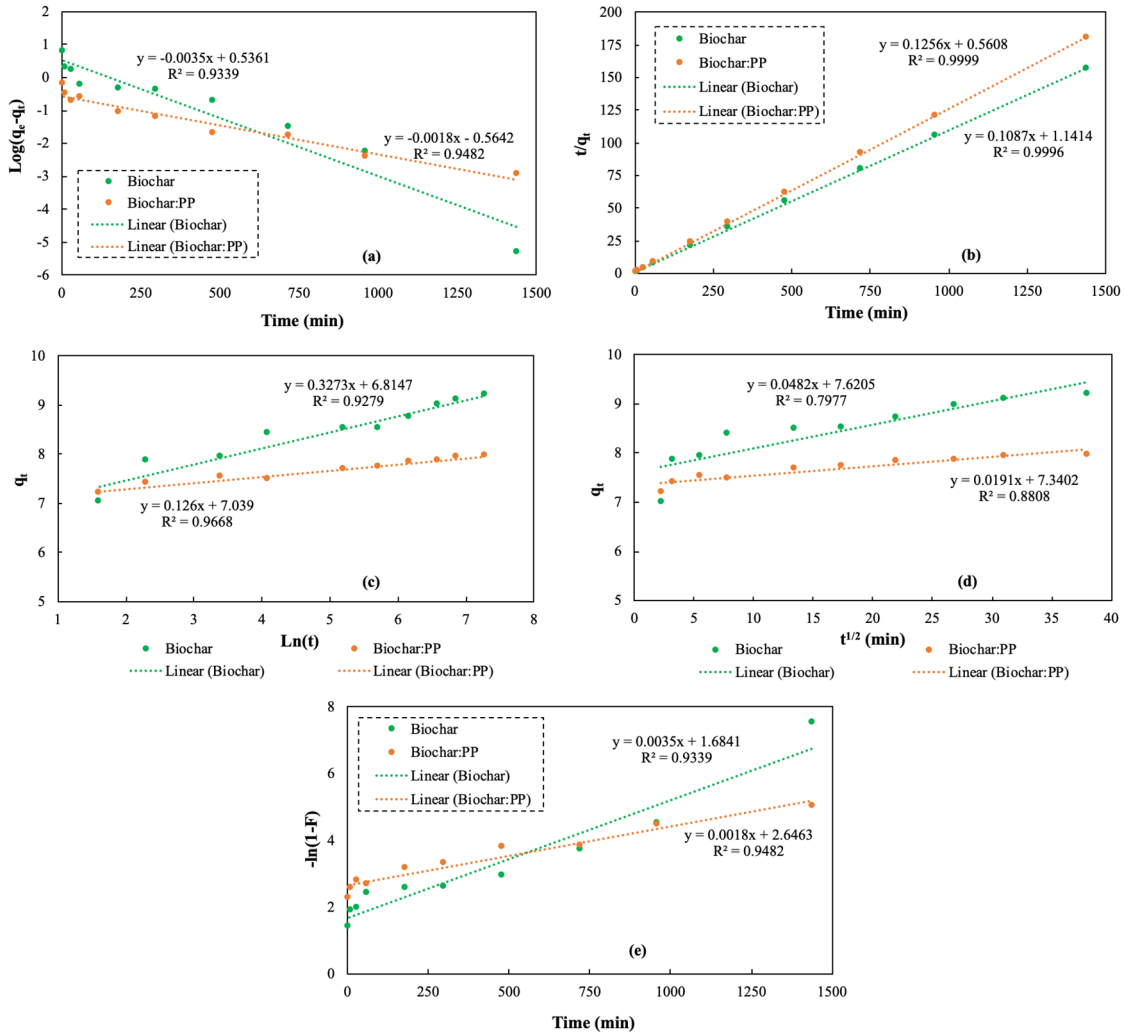

Fig. 9. Adsorption kinetic models for Cr(VI) adsorption on biochar and mixture of biochar and PP (1:1): (a) Pseudo-first order; (b) Pseudo-second order; (c) Elovich diffusion; (d) Intra-particle diffusion; (e) Liquid film diffusion.

Considering the mixture of biochar and PP microplastics, the coefficients of determination (R^2) of Redlich > Sips > Freundlich >> Langmuir. Langmuir's ARE value was higher than other models' ARE values, showing that the Langmuir model is not ideal for describing the adsorption equilibrium process. For the Sips model, $m_s = 1$ leads the model to return to the Langmuir equation; however, there is no agreement between the q_m of Sips and the $q_{experimental}$. For the Redlich-Peterson model, the coefficient $n = 0$ shows that the adsorption system has approached the Freundlich equation at high concentrations and poses a heterogeneous system [33].

G. Adsorption Kinetic

Table 3. Results of kinetic parameters for the adsorption of Cr(VI) onto biochar and mixture of biochar and PP (1:1)

Kinetic model	Parameters	Values	
		Biochar	Biochar:PP (1:1)
Pseudo-first order	$q_{e,\,cal}$ (mg/g)	1.71	0.57
	k_1 (min^{-1})	0.008	0.004
	R^2	0.93	0.95
Pseudo-second order	$q_{e,\,cal}$ (mg/g)	9.2	7.96
	k_2 (g/mg.min)	0.01	0.028
	h	0.88	1.78
	R^2	9.996×10^{-1}	9.999×10^{-1}
Elovich diffusion	α	3.6×10^{8}	2.29×10^{23}
	β	3.06	7.94
	R^2	0.93	0.97
Intra-particle diffusion	k_{id} ($mg/g.min^{-1/2}$)	0.048	0.019
	Intercept	7.62	7.34
	R^2	0.8	0.88
Liquid film diffusion	k_{fd} (min^{-1})	3.5×10^{-3}	1.8×10^{-3}
	Intercept	1.68	2.65
	R^2	0.93	0.95

The used kinetic models in this study are pseudo-first-order model (Fig. 9a), pseudo-second-order model (Fig. 9b), elovich diffusion (Fig. 9c), intra-particle diffusion model (Fig. 9d), and liquid film diffusion model (Fig. 9e). In additionally, Table 3 describes the kinetic parameters of Cr(VI) adsorption on biochar and the mixture of biochar and PP. All adsorption processes were well-fitted by both Pseudo-first-order and Pseudo-second-order models. However, the second-order kinetics model shows a better fit than the first-order kinetic model, as indicated by the higher correlation coefficient and the closer match between the calculated q_e value ($q_{e,\,cal}$) and the experimental q_e value ($q_{e,\,exp}$). The second-order kinetic model proposes that the rate-limiting step is a chemisorption process. This chemisorption may involve covalent forces through the sharing or exchange of electrons between the adsorbent and Cr(VI) ions or chemical bonding between Cr(VI) ions and polar functional groups such as aldehydes, acetone and acids on biochar [34, 35]. The second-order model also assumes that the adsorption rate depends on the adsorption capacity rather than the adsorbent concentration, and the adsorption is controlled by the available sites on the surface [35]. The results indicate that the initial adsorption rate (h) and the sorption rate constant (k_2) of Cr(VI) on biochar in the presence of PP were higher compared to biochar alone. This suggests that in the presence of PP, the adsorption of Cr(VI) occurs more rapidly and strongly due to surface interactions rather than the complex and slow sorption mechanism within the pores [15].

Elovich kinetic model proposes that the adsorbent surface is energetically heterogeneous for second-order kinetics. The high correlation coefficient of both processes ($R^2_{biochar\_Elovich} = 0.93$; $R^2_{biochar:PP\_Elovich} = 0.97$) indicate a good fit of the model. The α value of PP-presented biochar was higher than that of biochar, indicating a higher initial adsorption rate in the presence of PP. The β value also indicates stronger desorption in the presence of PP ($\beta_{biochar:PP} > \beta_{biochar}$).

Table 3 and Fig. 9d shows that the intra-particle diffusion model's R^2 values are consistently below 0.9, and their intercept values deviate from 0. Therefore, intra-particle diffusion is unsuitable for describing the Cr(VI) adsorption mechanism. Conversely, the R^2 value of the liquid film diffusion model for both processes was greater than 0.9, demonstrating that the transport of Cr(VI) molecules from the liquid phase to the solid phase plays a major role in the adsorption process.

V. Conclusions

The study shows that the appearance of PP microplastics has adverse impacts on Cr(VI) adsorption of biochar. Specifically, the co-existence of PP microplastics and biochar leads to (1) a shift in the optimal pH value of the adsorption, (2) a prolonging of the adsorption equilibration time, (3) a decrease in treatment efficiency as the mass of PP increases, (4) a reduction in the limit of optimal concentration of Cr(VI), (5) heterogeneous distribution of Cr(VI) on the surface of biochar and PP microplastics, (6) faster and stronger adsorption of Cr(VI), and (7) an acceleration of the desorption process. The adsorption mechanism of Cr(VI) onto biochar and microplastics is consistent with the Freundlich and Redlich-Peterson model, and the adsorption pathway was predicted with film diffusion as the main step of the adsorption process. In further studies, it is necessary to clarify the chemical transformation of the chromium state in the adsorption mechanism. It should also be tested under real conditions with a wastewater matrix. Finally, thorough research is necessary when applying the adsorption process to treat pollutants in the presence of microplastics, as their impacts on the treatment process are significant.

Conflict of Interest

The authors declare no conflict of interest.

Author Contributions

Ho Truong Nam Hai: project administration, conceptualization, methodology, funding acquisition, data curation, roles/writing original draft. Pham Thi Phuong Le: analysis. Nguyen Thao Nguyen: roles/writing original draft, visualization. Nguyen Thi Thanh Nhon: roles/writing original draft. Nguyen Tran Hanh Vy: analysis. Tan Le Hoang Doan: analysis. To Thi Hien: methodology, review and editing.

Funding

This research is funded by Vietnam National University, Ho Chi Minh City (VNU-HCM) under grant number C2022-

18-36. The authors thank the Air and Water pollution – Public Health – Climate Change research group of the Faculty of Environment, University of Science, VNUHCM for the support in this study. The authors also thank the Center for Innovative Materials & Architectures (INOMAR), Vietnam National University, Ho Chi Minh City for their support in using nitrogen adsorption.

REFERENCES

[1] J. Hubeny *et al.*, "Industrialization as a source of heavy metals and antibiotics which can enhance the antibiotic resistance in wastewater, sewage sludge and river water," *PLoS ONE*, vol. 16, no. 6, p. e0252691, Jun. 2021, doi: 10.1371/journal.pone.0252691.

[2] Md. A. Islam, M. J. Angove, and D. W. Morton, "Recent innovative research on chromium (VI) adsorption mechanism," *Environmental Nanotechnology, Monitoring & Management*, vol. 12, p. 100267, Dec. 2019, doi: 10.1016/j.enmm.2019.100267.

[3] Y. Wang, C. Peng, E. Padilla-Ortega, A. Robledo-Cabrera, and A. López-Valdivieso, "Cr(VI) adsorption on activated carbon: Mechanisms, modeling and limitations in water treatment," *Journal of Environmental Chemical Engineering*, vol. 8, no. 4, p. 104031, Aug. 2020, doi: 10.1016/j.jece.2020.104031.

[4] F. Liu, N. Nord, K. Bester, and J. Vollertsen, "Microplastics removal from treated wastewater by a biofilter," *Water*, vol. 12, no. 4, p. 1085, Apr. 2020, doi: 10.3390/w12041085.

[5] N. T. Nguyen, N. T. T. Nhon, H. T. N. Hai, N. D. T. Chi, and T. T. Hien, "Characteristics of microplastics and their affiliated PAHs in surface water in Ho Chi Minh City, Vietnam," *Polymers*, vol. 14, no. 12, p. 2450, Jun. 2022, doi: 10.3390/polym14122450.

[6] N. Oz, "Investigation of heavy metal adsorption on microplastics," *Appl. Ecol. Env.* Res., vol. 17, no. 4, 2019, doi: 10.15666/aeer/1704_73017310.

[7] J. Li, K. Zhang, and H. Zhang, "Adsorption of antibiotics on microplastics," *Environmental Pollution*, vol. 237, pp. 460–467, Jun. 2018, doi: 10.1016/j.envpol.2018.02.050.

[8] D. Brennecke, B. Duarte, F. Paiva, I. Caçador, and J. Canning-Clode, "Microplastics as vector for heavy metal contamination from the marine environment," *Estuarine, Coastal and Shelf Science*, vol. 178, pp. 189–195, Sep. 2016, doi: 10.1016/j.ecss.2015.12.003.

[9] Z. Long, W. Wang, X. Yu, Z. Lin, and J. Chen, "Heterogeneity and contribution of microplastics from industrial and domestic sources in a wastewater treatment plant in Xiamen, China," *Front. Environ. Sci.*, vol. 9, p. 770634, Nov. 2021, doi: 10.3389/fenvs.2021.770634.

[10] C. Schmid, L. Cozzarini, and E. Zambello, "Microplastic's story," *Marine Pollution Bulletin*, vol. 162, p. 111820, Jan. 2021, doi: 10.1016/j.marpolbul.2020.111820.

[11] A. Shakya and T. Agarwal, "Removal of Cr(VI) from water using pineapple peel derived biochars: Adsorption potential and re-usability assessment," *Journal of Molecular Liquids*, vol. 293, p. 111497, Nov. 2019, doi: 10.1016/j.molliq.2019.111497.

[12] J. Valentín-Reyes, R. B. García-Reyes, A. García-González, E. Soto-Regalado, and F. Cerino-Córdova, "Adsorption mechanisms of hexavalent chromium from aqueous solutions on modified activated carbons," *Journal of Environmental Management*, vol. 236, pp. 815–822, Apr. 2019, doi: 10.1016/j.jenvman.2019.02.014.

[13] D. E. Kimbrough, Y. Cohen, A. M. Winer, L. Creelman, and C. Mabuni, "A critical assessment of chromium in the environment," *Critical Reviews in Environmental Science and Technology*, vol. 29, no. 1, pp. 1–46, Jan. 1999, doi: 10.1080/10643389991259164.

[14] A. Waseem and J. Arshad, "A review of human biomonitoring studies of trace elements in Pakistan," *Chemosphere*, vol. 163, pp. 153–176, Nov. 2016, doi: 10.1016/j.chemosphere.2016.08.011.

[15] X. Li, X. Jiang, Y. Song, and S. X. Chang, "Coexistence of polyethylene microplastics and biochar increases ammonium sorption in an aqueous solution," *Journal of Hazardous Materials*, vol. 405, p. 124260, Mar. 2021, doi: 10.1016/j.jhazmat.2020.124260.

[16] F. Murphy, C. Ewins, F. Carbonnier, and B. Quinn, "Wastewater Treatment Works (WwTW) as a source of microplastics in the aquatic environment," *Environ. Sci. Technol.*, vol. 50, no. 11, pp. 5800–5808, Jun. 2016, doi: 10.1021/acs.est.5b05416.

[17] M. Simon, N. van Alst, and J. Vollertsen, "Quantification of microplastic mass and removal rates at wastewater treatment plants applying Focal Plane Array (FPA)-based Fourier Transform Infrared (FT-IR) imaging," *Water Research*, vol. 142, pp. 1–9, Oct. 2018, doi: 10.1016/j.watres.2018.05.019.

[18] F. G. Torres, D. C. Dioses-Salinas, C. I. Pizarro-Ortega, and G. E. De-la-Torre, "Sorption of chemical contaminants on degradable and non-degradable microplastics: Recent progress and research trends," *Science of The Total Environment*, vol. 757, p. 143875, Feb. 2021, doi: 10.1016/j.scitotenv.2020.143875.

[19] M.-A. Perea-Moreno, F. Manzano-Agugliaro, Q. Hernandez-Escobedo, and A.-J. Perea-Moreno, "Peanut shell for energy: properties and its potential to respect the environment," *Sustainability*, vol. 10, no. 9, p. 3254, Sep. 2018, doi: 10.3390/su10093254.

[20] J. Georgin, G. L. Dotto, M. A. Mazutti, and E. L. Foletto, "Preparation of activated carbon from peanut shell by conventional pyrolysis and microwave irradiation-pyrolysis to remove organic dyes from aqueous solutions," *Journal of Environmental Chemical Engineering*, vol. 4, no. 1, pp. 266–275, Mar. 2016, doi: 10.1016/j.jece.2015.11.018.

[21] E. A. Al-Maliky, H. A. Gzar, and M. G. Al-Azawy, "Determination of point of Zero Charge (PZC) of concrete particles adsorbents," *IOP Conf. Ser.: Mater. Sci. Eng.*, vol. 1184, no. 1, p. 012004, Sep. 2021, doi: 10.1088/1757-899X/1184/1/012004.

[22] A. Wiryawan, R. Retnowati, and R. Y. P. Burhan, "Method of analysis for determination of the Chromium (CR) species in water samples by spectrophotometry with diphenylcarbazide," *Journal of Environmental Engineering*, vol. 05, no. 01, p. 11, 2018.

[23] M. Thommes *et al.*, "Physisorption of gases, with special reference to the evaluation of surface area and pore size distribution (IUPAC Technical Report)," *Pure and Applied Chemistry*, vol. 87, no. 9–10, pp. 1051–1069, Oct. 2015, doi: 10.1515/pac-2014-1117.

[24] K.-W. Jung, M.-J. Hwang, K.-H. Ahn, and Y.-S. Ok, "Kinetic study on phosphate removal from aqueous solution by biochar derived from peanut shell as renewable adsorptive media," *Int. J. Environ. Sci. Technol.*, vol. 12, no. 10, pp. 3363–3372, Oct. 2015, doi: 10.1007/s13762-015-0766-5.

[25] Z. Movasaghi, S. Rehman, and Dr. I. ur Rehman, "Fourier Transform Infrared (FTIR) spectroscopy of biological tissues," *Applied Spectroscopy Reviews*, vol. 43, no. 2, pp. 134–179, Feb. 2008, doi: 10.1080/05704920701829043.

[26] S. C. Koay, S. Husseinsyah, and H. Osman, "Modified cocoa pod husk-filled polypropylene composites by using methacrylic acid," *BioResources*, vol. 8, no. 3, pp. 3260–3275, May 2013, doi: 10.15376/biores.8.3.3260-3275.

[27] T. Buruiana, E. C. Buruiana, V. Melinte, A. Colceriu, and M. Moldovan, "Urethane dimethacrylate oligomers for dental composite matrix: Synthesis and properties," *Polym. Eng. Sci.*, vol. 49, no. 6, pp. 1127–1135, Jun. 2009, doi: 10.1002/pen.21351.

[28] H. N. Tran *et al.*, "Adsorption mechanism of hexavalent chromium onto layered double hydroxides-based adsorbents: A systematic in-depth review," *Journal of Hazardous Materials*, vol. 373, pp. 258–270, Jul. 2019, doi: 10.1016/j.jhazmat.2019.03.018.

[29] T. D. Ntuli and V. E. Pakade, "Hexavalent chromium removal by polyacrylic acid-grafted *Macadamia* nutshell powder through adsorption–reduction mechanism: Adsorption isotherms, kinetics and thermodynamics," *Chemical Engineering Communications*, vol. 207, no. 3, pp. 279–294, Mar. 2020, doi: 10.1080/00986445.2019.1581619.

[30] B. Xu, F. Liu, P. C. Brookes, and J. Xu, "The sorption kinetics and isotherms of sulfamethoxazole with polyethylene microplastics," *Marine Pollution Bulletin*, vol. 131, pp. 191–196, Jun. 2018, doi: 10.1016/j.marpolbul.2018.04.027.

[31] B. Meroufel, O. Benali, M. Benyahia, Y. Benmoussa, and M. A. Zenasni, "Adsorptive removal of anionic dye from aqueous solutions by Algerian kaolin: Characteristics, isotherm, kinetic and thermodynamic studies," p. 10, 2013.

[32] F. A. Banat, B. Al-Bashir, S. Al-Asheh, and O. Hayajneh, "Adsorption of phenol by bentonite," Environmental *Pollution*, vol. 107, no. 3, pp. 391–398, Mar. 2000, doi: 10.1016/S0269-7491(99)00173-6.

[33] N. C. Le and D. Van Phuc, "Sorption of lead (II), cobalt (II) and copper (II) ions from aqueous solutions by γ -MnO_2 nanostructure," *Adv. Nat. Sci: Nanosci. Nanotechnol.*, vol. 6, no. 2, p. 025014, Mar. 2015, doi: 10.1088/2043-6262/6/2/025014.

[34] J. Wang and X. Guo, "Adsorption kinetic models: Physical meanings, applications, and solving methods," *Journal of Hazardous Materials*, vol. 390, p. 122156, May 2020, doi: 10.1016/j.jhazmat.2020.122156.

[35] H. Qiu, L. Lv, B. Pan, Q. Zhang, W. Zhang, and Q. Zhang, "Critical review in adsorption kinetic models," *J. Zhejiang Univ. Sci. A*, vol. 10, no. 5, pp. 716–724, May 2009, doi: 10.1631/jzus.A0820524.